Paper 265

©Civil-Comp Press, 2012
Proceedings of the Eleventh International Conference
on Computational Structures Technology,
B.H.V. Topping, (Editor),
Civil-Comp Press, Stirlingshire, Scotland

Numerical Analysis of Concrete at an Early Age

A. Ilc[1], G. Turk[2] and I. Planinc[2]
[1]Primorje d.d., Ajdovščina, Slovenia
[2]Faculty of Civil and Geodetic Engineering
University of Ljubljana, Slovenia

Abstract

A numerical procedure for modelling fully coupled thermal, hygral and mechanical behaviour of concrete at anearly age is presented. Concrete is treated as a porous material, composed of a solid skeleton and pores, filled with liquid water and moist air. Hydration of cement which causes temperature rise, desiccation and changes in porosity, permeability, stiffness and strength, is taken into account. A set of governing equations is solved iteratively by a finite element method. A numerical example is solved considering two different types of sorption isotherms. A comparison between experimental and numerical results shows the adequacy of the proposed procedure.

Keywords: early age concrete, numerical analysis, porous material, fully coupled problem, cement hydration, heat and mass transport, sorption isotherms.

1 Introduction

During the first days after casting concrete is subjected to drastic changes. Their main reason is hydration of cement, a chemical reaction during which water is combined with cement grains to form a solid cement structure. Whilst solidifying, concrete's physical properties are constantly changing: porosity and water content are decreasing while strength and modulus of elasticity are increasing. The reaction is exothermic and consequently it may lead to a significant temperature rise, depending on the geometry of concrete structure and the temperature of the surrounding media. Additionally, the hydration causes concrete desiccation which results in shrinkage. Both temperature gradient and shrinkage give rise to tension stresses. As tension strength of concrete is low, they have to be very limited to prevent cracking and ensure concrete durability.

A numerical modelling presents a possible and feasible method to address the described problem, but is rather complicated as concrete is a porous material composed of solid, liquid and gaseous phase. Thus the temperature disposition affects water, vapour and air flow and vice versa, the heat is transferred by moving liquids. Besides, both temperature and humidity have influence on concrete deformations and concrete displacements interfere with mass and heat movements. The last phenomenon is frequently neglected [1, 2], nevertheless, a fully coupled problem is considered in works of Gawin et al. [3, 4] and Davie et al. [5].

While most of the researchers concentrate on concrete after the hydration is almost completed, in work [1, 3, 4], a model adapted to concrete at early age is described. Its main advantage is that hydration of cement which causes temperature rise and desiccation of concrete is taken into account as an internal heat source. Besides, concrete strength, stiffness, permeability and porosity are modelled as ageing quantities.

The present paper follows the model presented in work [3, 4], but incorporates some different constitutive laws. Sorption isoterms are modelled according to the modified Davie's model [5] which enables their evaluation on the basis of water to cement ratio and eliminates the need for experiment, unavoidable in the formulation described in work [3]. Hydration of cement is described by a hydration curve, obtained by an adiabatic test and modelled by a mathematical function that is different from the one used in work [3].

Governing equations are expressed in terms of four primary state variables and solved iteratively by a finite element method. A numerical example dealing with adiabatic test is presented and discussed.

2 Balance equations

Presented balance equations are developed on the basis of hybrid mixture theory which was originally proposed by Hassanizadeh and Gray [6, 7, 8], applied for geomaterials by Lewis and Schrefler [9], and for early-age concrete by Gawin [3, 4].

Concrete is treated as a multi-phase porous material consisting of solid (marked s), liquid (w) and gaseous (g) phase. The last is assumed to behave as an ideal gas and is a mixture of dry air (ga) and water vapour (gw). First, mass balance equation is written for every constituent of concrete. For a constituent π, the equation reads:

$$\frac{\overset{\pi}{\mathrm{D}}\rho_\pi}{\mathrm{D}t} + \rho_\pi \mathrm{div}\mathbf{v}^\pi = \rho_\pi e^\pi(\rho), \tag{1}$$

where ρ_π is the apparent density, $\mathbf{v}^\pi$ the velocity and $\rho_\pi e^\pi(\rho)$ the volumetric mass source of a phase π.

Apparent density of the π phase is a product of its intrinsic density ρ^π and volumetric portion. If concrete porosity n is defined as a volumetric portion of pores, the volumetric portion of solid skeleton η^s can be expressed as $(1 - n)$. The volumetric portion of liquid and gaseous phase are determined as nS_w and $n(1 - S_w)$, where S_w is a degree of saturation of the pores with liquid water.

If m_{hydr} is the mass of water in a cubic metre of concrete, then $\dot{m}_{hydr}$ is the mass sink of liquid water and a mass source of solid skeleton. Similarly, $\dot{m}_{vap}$ is the mass source of water vapour and the mass sink of liquid water, where m_{vap} is the volumetric mass of evaporating water.

Regarding all given relations and definitions, four mass balance equations can be written for solid skeleton, liquid water, water vapour and dry air. It turns out that $\overset{s}{\mathrm{D}}n/\mathrm{D}t$ can be expressed from the equation for the solid skeleton and inserted in the other equations, and $\dot{m}_{vap}$ can be expressed from the equation for liquid water and inserted in the equation for water vapour. In this way, four governing equations reduce to two mass balance equations:

$$
\begin{aligned}
&\frac{(1-n)(1-S_w)\rho^{ga}}{\rho^s}\frac{\overset{s}{\mathrm{D}}\rho^s}{\mathrm{D}t} + n(1-S_w)\frac{\overset{s}{\mathrm{D}}\rho^{ga}}{\mathrm{D}t} - n\rho^{ga}\frac{\overset{s}{\mathrm{D}}S_w}{\mathrm{D}t} + (1-S_w)\rho^{ga}\mathrm{div}\mathbf{v}^s + \\
&\qquad \mathrm{div}\left(\mathbf{J}_d^{ga}\right) + \mathrm{div}\left(n(1-S_w)\rho^{ga}\mathbf{v}^{gs}\right) = \frac{(1-S_w)\rho^{ga}}{\rho^s}\dot{m}_{hydr},
\end{aligned}
$$

$$
\begin{aligned}
&\frac{(1-n)((1-S_w)\rho^{gw} + S_w\rho^w)}{\rho^s}\frac{\overset{s}{\mathrm{D}}\rho^s}{\mathrm{D}t} + nS_w\frac{\overset{s}{\mathrm{D}}\rho^w}{\mathrm{D}t} + n(1-S_w)\frac{\overset{s}{\mathrm{D}}\rho^{gw}}{\mathrm{D}t} + \\
&\qquad n(\rho_w - \rho_{gw})\frac{\overset{s}{\mathrm{D}}S_w}{\mathrm{D}t} + (\rho_w S_w + \rho_{gw}(1-S_w))\mathrm{div}\mathbf{v}^s + \mathrm{div}\left(\mathbf{J}_d^{gw}\right) + \\
&\qquad \mathrm{div}\left(n(1-S_w)\rho^{gw}\mathbf{v}^{gs}\right) + \mathrm{div}\left(nS_w\rho^w\mathbf{v}^{ws}\right) = \frac{S_w\rho^w + (1-S_w)\rho^{gw} - \rho^s}{\rho^s}\dot{m}_{hydr},
\end{aligned}
\tag{2}
$$

where the dry air velocity $\mathbf{v}^{ga}$ is decomposed into the advective $\mathbf{v}^g$ and diffusive part $\mathbf{u}^{ga}$, which is described by the diffusive mass flux $\mathbf{J}_d^{ga}$. As gas is an ideal mixture of dry air and water vapour, the following equation holds:

$$
\mathbf{J}_d^{ga} = n(1-S_w)\rho^{ga}\mathbf{u}^{ga} = -\mathbf{J}_d^{gw} = n(1-S_w)\rho^{gw}\mathbf{u}^{gw}. \tag{3}
$$

Second group of balance equations are energy balance equations. After assuming that, at any given point, all concrete constituents have the same temperature T, and neglecting viscous dissipation and mechanical work, caused by density variations and volume fraction changes, the energy balance equations for all concrete phases are summed up which results in one energy balance equation:

$$
\begin{aligned}
&(\rho C_p)_{\mathrm{eff}}\frac{\overset{s}{\mathrm{D}}T}{\mathrm{D}t} + \left(nS_w\rho^w C_p^w\mathbf{v}^{ws} + n(1-S_w)\rho^g C_p^g\mathbf{v}^{gs}\right)\mathrm{grad}T + \mathrm{div}\mathbf{q} - \\
&\qquad \rho_w S_w\mathrm{div}\mathbf{v}^s\Delta H_{vap} - \left(\frac{(1-n)S_w\rho^w}{\rho^s}\frac{\overset{s}{\mathrm{D}}\rho^s}{\mathrm{D}t} + nS_w\frac{\overset{s}{\mathrm{D}}\rho^w}{\mathrm{D}t}\right)\Delta H_{vap} - \\
&\qquad n\rho_w\frac{\overset{s}{\mathrm{D}}S_w}{\mathrm{D}t}\Delta H_{vap} - \mathrm{div}\left(nS_w\rho^w\mathbf{v}^{ws}\right)\Delta H_{vap} = \dot{m}_{hydr}\Delta H_{hydr} - \frac{S_w\rho^w - \rho^s}{\rho^s}\Delta H_{vap},
\end{aligned}
\tag{4}
$$

where $\triangle H_{hydr}$ is the specific heat of hydration, $\triangle H_{vap}$ is the specific heat of water evaporation, q is the heat flux, C_p^π is the specific heat of the phase π and the heat capacity $(\rho C_p)_{\text{eff}}$ is:

$$(\rho C_p)_{\text{eff}} = (1-n)\rho^s C_p^s + nS_w\rho^w C_p^w + n(1-S_w)\rho^g C_p^g. \tag{5}$$

Similarly as energy equation, the linear momentum balance equation is obtained by summing up the equations for all four constituents. If neglecting inertial forces, this equation reads as:

$$\text{div}\sigma + \rho\text{g} = 0, \tag{6}$$

where σ is the total stress, g the gravitational acceleration and ρ the density of concrete which can be evaluated from:

$$\rho = \rho_s + \rho_w + \rho_g = (1-n)\rho^s + nS_w\rho^w + n(1-S_w)\rho^g. \tag{7}$$

3 Constitutive equations

3.1 Hydration of cement

Hydration of cement is a chemical reaction, during which cement grains react with water and, together with aggregate, create increasingly rigid structure. Because the reaction is exothermic, heat is released during its progress. This heat can be measured with the adiabatic test and described by the adiabatic curve, which shows temperature increase in concrete due to the hydration in completely isolated (adiabatic) conditions.

A hydration degree Γ_{hydr} is defined as a ratio between the mass of hydrated (chemically combined) water m_{hydr} and the mass of hydrated water at finished hydration m_{hydr}^∞. Assuming the specific heat of hydration being constant during the whole course of hydration, the hydration degree can be further expressed as a ratio between the heat of hydration Q_{hydr} and the total heat of hydration Q_{hydr}^∞.

$$\Gamma_{hydr} = \frac{m_{hydr}}{m_{hydr}^\infty} = \frac{m_{hydr}\Delta H_{hydr}}{m_{hydr}^\infty \Delta H_{hydr}} = \frac{Q_{hydr}}{Q_{hydr}^\infty}. \tag{8}$$

Neglecting change of the heat capacity during adiabatic test $(\rho C_p)^{ad}$, the hydration degree is:

$$\Gamma_{hydr}^{ad} = \frac{T^{ad}}{T_\infty^{ad} - T_0^{ad}}, \tag{9}$$

where T^{ad} is the experimentally determined adiabatic curve and T_∞^{ad} and T_0^{ad} are the final and the initial temperature of the adiabatic test, respectively.

Since the chemical reaction runs faster at higher temperatures, the adiabatic curve needs to be corrected by Arrhenius function [1, 3] if the temperature does not follow the same adiabatic temperature rise. The rate of hydration degree then reads as:

$$\dot{\Gamma}_{hydr} = \frac{\dot{T}^{ad}}{T_{\infty}^{ad} - T_{0}^{ad}} \exp\left(\frac{E_a}{R \frac{(\rho C_p)^{ad} T^{ad}}{(\rho C_p)}} \right) \exp\left(-\frac{E_a}{RT} \right), \tag{10}$$

where E_a is the activation energy and R is the universal gas constant.

To simplify its numerical evaluation, the adiabatic curve is approximated by a mathematical function. The function proposed by [10] with the material parameters a_a, b_a, c_a and d_a is used here:

$$T^{ad} = a_a + b_a \exp\left(-(c_a/t)^{d_a} \right). \tag{11}$$

The hydration rate is effected not only by the concrete temperature but also by the moisture content which is affected by the relative humidity of the air in concrete pores defined as a ratio between the actual and saturated water vapour pressure p^{gw}/p^{gws}. To evaluate the influence of moisture content on hydration rate, it is multiplied by an expression with the material parameter a_h:

$$\beta_{\varphi} = \left(1 + a_h^4 \left(1 - \frac{p^{gw}}{p^{gws}} \right)^4 \right)^{-1}. \tag{12}$$

To evaluate $\dot{m}_{hydr}$ from the equation (8), a mass of chemically combined water at completed hydration m_{hydr}^{∞} needs to be known. If there is enough water in the concrete mixture so that entire cement is able to react, then 23 g of water is combined with 100 g of cement [11]. Because this condition is rarely fulfilled, this value is multiplied by κ_{∞}, which is defined as

$$\kappa_{\infty} = \frac{1.031 w/c}{0.194 + w/c}, \tag{13}$$

where w/c is the water to cement ratio. If the apparent density of cement is denoted m_{cem}, $\dot{m}_{hydr}$ can be expressed as:

$$\dot{m}_{hydr} = m_{hydr}^{\infty} \dot{\Gamma}_{hydr} = 0.23 \kappa_{\infty} m_{cem} \dot{\Gamma}_{hydr}. \tag{14}$$

The specific hydration heat can be evaluated from the equations (8 – 14) as:

$$\triangle H_{hydr} = \frac{(\rho C_p)^{ad} T^{ad}}{m_{hydr}^{\infty}}. \tag{15}$$

3.2 Porosity

Concrete is a highly porous material with many pores of different diameter, the diameter being a typical dimension of the cross section of the pore. Pores with the diameter smaller than 0.01 μm, are gel pores and are filled with gel water, which is physically bound to the cement gel and thus it is a part of concrete's solid skeleton. Pores with diameter greater than 0.01 $\mu\mathrm{m}$ are capillary pores and the capillary porosity is defined as a volumetric portion of capillary pores in concrete.

During the course of hydration reaction, concrete is more and more dense and its porosity is reducing. Several authors use different models to describe the change of porosity of the cement paste, induced by the progress of hydration. In general, they can be all expressed as:

$$n = n_0 - n_1 \Gamma_{hydr}, \tag{16}$$

where n_0 (initial porosity) and n_1 are constants, dependant on water to cement ratio (w/c). For $w/c = 0.45$, initial porosity is about 0.59 and n_1 ranges from 0.33 to 0.39 [3, 11, 12]. As these are values for the cement paste, some researchers multiply them by a portion of the cement paste in concrete [13, 14], while the others equal the porosity of concrete to the porosity of cement paste [3].

3.3 Densities, pressures and molar masses

The intrinsic density of liquid water depends on its temperature and is evaluated from:

$$\rho^w = \rho^{w_0}(1 - \beta_w T), \tag{17}$$

where $\rho^{w_0} = 999,84$ kg/m^3 is the water density at $0\,^\circ\mathrm{C}$ and $\beta_w = 207 \cdot 10^{-6}/\,^\circ\mathrm{C}$ is the thermal dilatation coefficient of water. In this and in the following equations, temperature T is in $^\circ\mathrm{C}$.

Analogously, the intrinsic density of solid skeleton is:

$$\rho^s = \rho^{s_0}(1 - \beta_s T). \tag{18}$$

The capillary pressure is defined as a difference between the pressure of gaseous phase p^g and liquid phase p^w [9]:

$$p^c = p^g - p^w. \tag{19}$$

Gaseous phase is a binary mixture of two ideal gasses: dry air and water vapour. Therefore, the following relation holds:

$$p^{ga} = p^g - p^{gw}, \tag{20}$$

where p^{ga} and p^{gw} are the partial pressures of dry air and water vapour. The last one can be evaluated by Kelvin's law:

$$p^{gw} = p^{gws} \exp\left(-\frac{p^c}{\rho^w} \frac{M_w}{R(T+273)} \right), \tag{21}$$

where $M_w = 18$ kg/kmol is the molar mass of water and p^{gws} is the saturated water pressure which can be evaluated from:

$$p^{gws} = 618.8710^{-\frac{7.5T}{T+237}}, \tag{22}$$

where the pressure p^{gws} is in Pa.

Because the air is assumed to be an ideal gas, $\rho^g = \rho^{ga} + \rho^{gw}$ holds. The density of the ideal gas π depends on its pressure, temperature and molar mass:

$$\rho^\pi = \frac{p^\pi M_\pi}{(T + 273)R}. \tag{23}$$

If the molar mass of dry air is denoted as $M_a = 29$ kg/kmol, then the molar mass of humid air M_g is:

$$M_g = \left(\frac{\rho^{gw}}{\rho^g M_w} + \frac{\rho^{ga}}{\rho^g M_a}\right)^{-1}. \tag{24}$$

3.4 Sorption isotherm

The sorption isotherms describe relationship between moisture content and relative humidity of the air in pores. Gawin et al. [3] apply the rule suggested by Baroghel-Bouny et al. [15]:

$$S_w = \left(1 + \left(\frac{p^c}{a_s}\right)^{b_s/(b_s-1)}\right)^{-1/b_s}, \tag{25}$$

where a_s and b_s are material parameters which must be experimentally determined for every concrete mixture and for the whole temperature range to be modelled. As these experiments are difficult to conduct, Davie et al. [5] propose another expression:

$$\begin{aligned} nS_w &= \begin{cases} \frac{m_{cem}}{\rho^w}\left(\frac{n_0\rho_0^w}{m_{cem}}\frac{p^{gw}}{p^{gws}}\right)^{1/m} & \text{for } \frac{p^{gw}}{p^{gws}} \leq 0.96 \\ a\left(\frac{p^{gw}}{p^{gws}}\right)^3 + b\left(\frac{p^{gw}}{p^{gws}}\right)^2 + c\frac{p^{gw}}{p^{gws}} + d & \text{for } 0.96 < \frac{p^{gw}}{p^{gws}} < 1 \\ n & \text{for } \frac{p^{gw}}{p^{gws}} = 1 \end{cases}, \\ m &= 1.04 - \frac{(T+10)^2}{(T+10)^2 + 22.3(25+10)^2}, \end{aligned} \tag{26}$$

where ρ_0^w is the initial water density and a, b, c and d are parameters, determined in a way that S_w is a continuously differentiable function of p^{gw}/p^{gws}. Using a polynomial to bridge the gap between 96% and 100% of relative humidity can result in saturation degree greater than 1, which is physically impossible and causes numerical problems. Therefore, this expression is replaced by:

$$S_w = 1 - c\exp\left(-a\left(\frac{1}{1 - p^{gw}/p^{gws}}\right)^b\right), \tag{27}$$

where a, b and c are parameters, determined in a way that S_w is a continuous and differentiable function of p^{gw}/p^{gws} which reaches value 1 at $p^{gw}/p^{gws} = 1$.

3.5 Fluids flow and diffusion

Even if the structure of concrete is very complex, as the size of pores ranges from micropores to cracks, the average fluid flow can be still described by Darcy's law:

$$nS_\pi \mathbf{v}^{\pi s} = -\frac{k^{r\pi}\mathbf{k}}{\mu^\pi}\left(\mathrm{grad} p^\pi - \rho^\pi \mathbf{g}\right), \tag{28}$$

where π is air (g) or water (w), $S_g = 1 - S_w$ is the saturation degree of pores with air, $\mathbf{k}$ is the intrinsic permeability tensor, $k^{r\pi}$ and μ^π denote relative permeability and dynamic viscosity of air and liquid water and can be evaluated from [16, 17]:

$$k^{rw} = \sqrt{S_w}\left(1 - \left(1 - S_w^{1/m}\right)^m\right)^2, \tag{29}$$

$$k^{rg} = \sqrt{1 - S_w}\left(1 - S_w^{1/m}\right)^{2m}, \tag{30}$$

$$\mu_w = 0.6612(T + 44.15)^{-1.562}, \tag{31}$$

$$\mu_g = \mu_{gw} + \left(\mu_{ga} - \mu_{gw}\right)\left(\frac{p^{ga}}{p^g}\right)^{0.608}, \tag{32}$$

$$\mu_{gw} = 8.85 \cdot 10^{-6} + 3.53 \cdot 10^{-8}T, \tag{33}$$

$$\mu_{ga} = 17.17 \cdot 10^{-6} + 4.73 \cdot 10^{-8}T + 2.22 \cdot 10^{-11}T^2, \tag{34}$$

where the dynamic viscosity μ_π is in Pa s, m is $1/b$, where b is 2.27 for ordinary and 2.06 for high-strength concrete [15]. The presented model neglects influence of cracks which appear due to large tensile stresses.

Fick's law describes diffusion of dry air and water vapour in the gaseous phase [3, 9, 17]:

$$\mathbf{J}_d^{gw} = -\rho^g \mathbf{D}_d^{gw} \mathrm{grad}\left(\frac{\rho^{gw}}{\rho^g}\right), \tag{35}$$

where $\mathbf{D}_d^{gw}$ is the effective diffusivity tensor of vapour in the air and may be evaluated from [15, 17]:

$$\mathbf{D}_d^{gw} = \mathbf{D}_d^{ga} = n(1 - S_w)1.87 \cdot 10^{-5}\frac{(T + 273)^{2.072}}{p^g}\frac{\delta}{\tau^2}, \tag{36}$$

where $\delta = 0.5$ and $\tau = 3$.

3.6 Heat conduction

The specific heat of dry air, liquid water and water vapour, are determined by the following equations (specific heat is in J/kg °C) [17]:

$$C_p^{ga} = a(T + 273)^3 + b(T + 273)^2 + c(T + 273) + d, \tag{37}$$

where $a = -9.8494 \cdot 10^{-8}$, $b = 3.5644 \cdot 10^{-4}$, $c = -1.2162 \cdot 10^{-1}$ and $d = 1.0125 \cdot 10^{3}$,

$$C_p^{gw} = 7.1399(T + 273) - 443 + \left(\frac{a(T + 273)}{513.15}\right)^b, \tag{38}$$

where $a = 1.1377$ and $b = 29.444$,

$$C_p^{w} = 2.4768(T + 273) + 3368.2 + \left(\frac{a(T + 273)}{513.15}\right)^b, \tag{39}$$

where $a = 1.0854$ and $b = 31.445$.

The specific heat of evaporation of water $\vartriangle H_{vap}$ is assumed to be constant and has the value of $2.26 \cdot 10^6$ J/kg.

To model the heat conduction through concrete, Fourier's law is used in the following form:

$$\mathbf{q} = -\lambda_{\mathit{eff}}\, \mathrm{grad} T, \tag{40}$$

where λ_{eff} is the effective thermal conductivity.

3.7 Principle of effective stresses and deformation

Concrete is composed of the solid skeleton and the pores filled with air and water. The total stress $\boldsymbol{\sigma}$ which is in balance with external load is the sum of the stress of the solid skeleton (effective stress) $\boldsymbol{\sigma}^{\mathit{eff}}$ and the pressure exerted on the skeleton by pore liquids p^s:

$$\boldsymbol{\sigma} = \boldsymbol{\sigma}^{\mathit{eff}} - p^s \mathbf{I}, \tag{41}$$

where $\mathbf{I}$ is $[1\ 1\ 1\ 0\ 0\ 0]^{\mathrm{T}}$. The stresses $\boldsymbol{\sigma}$ and $\boldsymbol{\sigma}^{\mathit{eff}}$ are positive in tension, while the pressure p^s is positive in compression. Vectors of stresses (and deformations) have the form:

$$\boldsymbol{\sigma} = \begin{bmatrix} \sigma^{xx} & \sigma^{yy} & \sigma^{zz} & \sigma^{xy} & \sigma^{xz} & \sigma^{yz} \end{bmatrix}^{\mathrm{T}}. \tag{42}$$

If χ^{ws} is the portion of the solid skeleton's surface which is in contact with water then p^s reads as:

$$p^s = p^g - p^{atm} - \chi^{ws} p^c. \tag{43}$$

For geomaterials, $\chi^{ws} = S_w$ is usually valid, but this relation is not appropriate for the concrete because it has a large portion of very thin pores and huge internal surface. Therefore, the connection $\chi^{ws}(S_w)$ is established in work [4] on the basis of experimental results obtained by Baroghel-Bouny et al. [15] and it is approximated by the following function (for the ordinary concrete):

$$\chi^{ws} = 0.1759 \exp\left(-\left(\frac{0.1463}{S_w}\right)^{1.391}\right). \tag{44}$$

Total deformation of the concrete skeleton $\boldsymbol{\epsilon}_{tot}$ can be decomposed in:

$$\boldsymbol{\epsilon}_{tot} = \boldsymbol{\epsilon}_e + \boldsymbol{\epsilon}_c + \boldsymbol{\epsilon}_t + \boldsymbol{\epsilon}_{ch}, \tag{45}$$

where $\boldsymbol{\epsilon}_e$ is the elastic deformation caused by external load and drying, $\boldsymbol{\epsilon}_c$ is the deformation because of the creep, $\boldsymbol{\epsilon}_t$ is the deformation due to changes in the temperature and ϵ_{ch} are the deformation on the account of chemical shrinkage. Deformations which are the result of cracking are not considered. Because elastic deformation is in correlation with effective stress, which is influenced by the change in relative humidity, it includes drying shrinkage.

If E is the modulus of elasticity, dependant on the hydration degree, the following holds:

$$\mathrm{d}\boldsymbol{\sigma}^{\text{eff}} = E\,\mathbf{D}\,\mathrm{d}\boldsymbol{\epsilon}_e + \mathrm{d}E\,\mathbf{D}\,\boldsymbol{\epsilon}_e \tag{46}$$

where $\mathbf{D}$ is the stiffness tensor with an inverse $\mathbf{G}$. If ν is the Poisson's ratio, it reads for three dimensional state as:

$$\mathbf{D} = \mathbf{G}^{-1} = \begin{bmatrix} 1-\nu & \nu & \nu & 0 & 0 & 0 \\ \nu & 1-\nu & \nu & 0 & 0 & 0 \\ \nu & \nu & 1-\nu & 0 & 0 & 0 \\ 0 & 0 & 0 & (1-2\nu)/2 & 0 & 0 \\ 0 & 0 & 0 & 0 & (1-2\nu)/2 & 0 \\ 0 & 0 & 0 & 0 & 0 & (1-2\nu)/2 \end{bmatrix}. \tag{47}$$

The deformation caused by a change of temperature is:

$$\mathrm{d}\boldsymbol{\epsilon}_t = \beta_s/3\,\mathrm{d}T\,\mathbf{I}. \tag{48}$$

Impact of the chemical shrinkage may be expressed by:

$$\mathrm{d}\boldsymbol{\epsilon}_{ch} = \beta_{ch}/3\,\mathrm{d}\Gamma_{hydr}\,\mathbf{I}, \tag{49}$$

where β_{ch} is a material parameter.

Modelling of creep is based on the Bažant's formulation [19, 20], where creep deformation is composed of a viscoelastic part, described by a Kelvin's chain and dependant on the hydration degree, and viscous part, describing the long term creep which takes place even if the hydration has already finished. Presented model follows the one represented by Gawin et al. [4] who connected creep with effective instead of total stress. The total creep may be evaluated from the following algorithm [23]:

$$\begin{aligned}
&{}_{\Delta}\boldsymbol{\epsilon}_c = \frac{\mathbf{G}_{\Delta}\boldsymbol{\sigma}^{\mathit{eff}}}{E''} + {}_{\Delta}\boldsymbol{\epsilon}''_c,\\
&\frac{1}{E''} = \frac{1}{v^{i+1/2}}\sum_{\mu=1}^{N}\frac{1-\lambda_\mu}{E_\mu},\\
&{}_{\Delta}\boldsymbol{\epsilon}''_c = R_T(T^{i+1/2})F(\boldsymbol{\sigma}^{\text{eff},i+1/2})\\
&\qquad\left[\frac{1}{v^{i+1/2}}\sum_{\mu=1}^{N}(1-\exp(-{}_{\Delta}y_\mu))\left(\frac{\mathbf{G}\boldsymbol{\sigma}^{\mathit{eff},i}}{E_\mu}-\boldsymbol{\gamma}^i_\mu\right)+2c_cS^{i+1}\mathbf{G}\boldsymbol{\sigma}^{\mathit{eff},i}{}_{\Delta}t\right],\\
&\boldsymbol{\gamma}^{i+1}_\mu = \boldsymbol{\gamma}^i_\mu\exp(-{}_{\Delta}y_\mu)+\frac{\mathbf{G}\boldsymbol{\sigma}^{\mathit{eff},i}}{E_\mu}(1-{}_{\Delta}y_\mu)+\frac{1-\lambda_\mu}{E_\mu}\mathbf{G}_{\Delta}\boldsymbol{\sigma}^{\mathit{eff}},\\
&{}_{\Delta}y_\mu = \frac{{}_{\Delta}t}{\tau_\mu},\qquad \lambda_\mu = \frac{1-\exp(-{}_{\Delta}y_\mu)}{{}_{\Delta}y_\mu},
\end{aligned} \tag{50}$$

where $v = \Gamma_{hydr}$, E_μ are coefficients of the Kelvin's chain and are evaluated in the sense of continuous retardation spectrum ($\bar{f}_c$ is an average 28-day compression strength in MPa) [22]:

$$\begin{aligned}
&A_\mu = \frac{1}{E_\mu} = L(\tau_\mu)\Delta(\ln\tau_\mu),\qquad \tau_{\mu+1} = 10\tau_\mu,\\
&L(\tau) = \left(\frac{-2n^2(3\tau)^{2n-3}(n-1-(3\tau)^n)}{(1+(3\tau)^n)^3}\right.\\
&\qquad\left.+\frac{n(n-2)(3\tau)^{n-3}(n-1-(3\tau)^n)-n^2(3\tau)^{2n-3}}{(1+(3\tau)^n)^2}\right)\frac{(3\tau)^3}{2}q_2,\\
&n = 0.1,\qquad \lambda_0 = 1\text{ day},\qquad q_2 = 185.4m^{0.5}_{cem}\bar{f}_c^{-0.9},
\end{aligned} \tag{51}$$

S^{i+1} is concrete microprestress [20]:

$$S^{i+1} = \frac{S^i - c_1\omega\Delta(\ln h)}{1+c_0S_i\omega\Delta t}, \tag{52}$$

where c_1 and c_0 are material parameters, $h = p^{gw}/p^{gws}$ is relative humidity of the air in pores and:

$$\omega = \begin{cases} (\tan{}_{\Delta}\xi)/{}_{\Delta}\xi & \text{for } {}_{\Delta}h > 0 \text{ in } {}_{\Delta}\xi > 10^{-5},\\ (\tanh{}_{\Delta}\xi)/{}_{\Delta}\xi & \text{for } {}_{\Delta}h < 0 \text{ in } {}_{\Delta}\xi > 10^{-5},\\ 1 & \text{for } {}_{\Delta}\xi < 10^{-5}; \end{cases}\qquad {}_{\Delta}\xi = \sqrt{c_0c_1{}_{\Delta}t|{}_{\Delta}\ln h|}. \tag{53}$$

$F(\boldsymbol{\sigma}^{\text{eff},i+1/2})$ and $R_T(T^{i+1/2})$ give consideration to the influence of high stress and temperature on creep and read as [23, 24]:

$$F(\sigma(t)) = \frac{1+s^2}{1-s^{10}},\qquad s = \frac{\sigma(t)}{\bar{f}_c}, \tag{54}$$

$$R_T = \exp\left(\frac{U'_c}{R}\left(\frac{1}{T_0}-\frac{1}{T_0}\right)\right),\quad T_0 = 293K,\quad \frac{U'_c}{R} = 0.18\cdot 110m_w^{-0.27}\bar{f}_c^{0.54}. \tag{55}$$

4 System of governing equations and its solving

To solve four equations (2, 4, 6), four state variables need to be chosen. The choice of displacement vector $\boldsymbol{u}$, temperature T and gas pressure p^g is somehow obvious while the selection of the variable to describe moisture state is more difficult. As suggested by Gawin et al. [3, 4], the last variable is capillary pressure, its meaning being formally generalised to cover complete range of moisture in pores [3].

After inserting constitutive equations in the balance equations and thus expressing them with the chosen state variables, discretization in space is carried out by means of the finite elements method. The principle of virtual work is implied to get the system of governing equations in the following form:

$$\begin{bmatrix} \boldsymbol{C}_{gg} & \boldsymbol{C}_{gc} & \boldsymbol{C}_{gt} & \boldsymbol{C}_{gu} \\ 0 & \boldsymbol{C}_{cc} & \boldsymbol{C}_{ct} & \boldsymbol{C}_{cu} \\ 0 & \boldsymbol{C}_{tc} & \boldsymbol{C}_{tt} & \boldsymbol{C}_{tu} \\ \boldsymbol{C}_{ug} & \boldsymbol{C}_{uc} & \boldsymbol{C}_{ut} & \boldsymbol{C}_{uu} \end{bmatrix} \begin{bmatrix} \dot{p}^g \\ \dot{p}^c \\ \dot{T} \\ \dot{\boldsymbol{u}} \end{bmatrix} + \begin{bmatrix} \boldsymbol{K}_{gg} & \boldsymbol{K}_{gc} & \boldsymbol{K}_{gt} & 0 \\ \boldsymbol{K}_{cg} & \boldsymbol{K}_{cc} & \boldsymbol{K}_{ct} & 0 \\ \boldsymbol{K}_{tg} & \boldsymbol{K}_{tc} & \boldsymbol{K}_{tt} & 0 \\ \boldsymbol{K}_{ug} & \boldsymbol{K}_{uc} & \boldsymbol{K}_{ut} & \boldsymbol{K}_{uu} \end{bmatrix} \begin{bmatrix} p^g \\ p^c \\ T \\ \boldsymbol{u} \end{bmatrix} = \begin{bmatrix} \boldsymbol{f}_g \\ \boldsymbol{f}_c \\ \boldsymbol{f}_T \\ \boldsymbol{f}_{\boldsymbol{u}} \end{bmatrix}, \tag{56}$$

where $\boldsymbol{C}_{ij}$, $\boldsymbol{K}_{ij}$ and $\boldsymbol{f}_i$ are dependant on p^g, p^c, T and $\boldsymbol{u}$ which is why the system has to be solved iteratively.

5 Numerical example

To validate presented numerical procedure, a numerical model of adiabatic test conducted by Bentz et al. [25] is made and the results are compared to the experiment and to those obtained by Gawin et al. [3].

A specimen is a 60 cm long concrete cylinder with a diameter of 4 cm. It is sealed and thermally isolated. Because the length of cylinder is much larger than its radius, only a slice of it is modelled. Considering axial symmetry of the specimen, the problem is one dimensional and is modelled by 26 four-node isoparametric axially symmetric finite elements, whose length diminishes towards the surface (Figure 1).

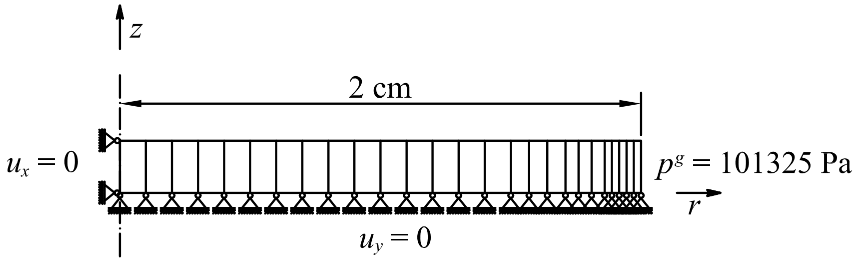

Figure 1: Finite elements mesh and boundary conditions for the example

The initial temperature of the concrete is 20 °C, the initial relative humidity is

99.9% and the initial hydration degree 0.1. Material parameters of concrete are summarized in Table 1.

Parameter	Symbol	Value	Unit
Water / cement ratio	w/c	0.45	
Cement content	m_{cem}	420	kg/m^3
Porosity	n	30.6	%
Intrinsic permeability	k	$3 \cdot 10^{-18}$	m^2
Apparent density	ρ_{eff}	2285	kg/m^3
Specific heat	$C_{p,\text{eff}}$	1020	J/kgK
Thermal conductivity	λ_{eff}	1.5	W/mK
Thermal dilatation coefficient	β_s	$3.6 \cdot 10^{-5}$	1/K
Young modulus	E	24.11	GPa
Poison's ratio	μ	0.2	
Compressive strength	f_c	26	MPa
Parameters in (11)	a_a	0	°C
	b_a	40	°C
	c_a	72000	s
	d_a	2.5	
Parameter in (12)	a_h	5	
Activation energy	E_a	41570	K
Parameters in (25)	a_s	25.4	MPa
	b_s	1.8	
Parameter in (50)	c_c	$13.55 \cdot 10^{-9}$	$1/$MPa^2 s
Parameters in (52)	c_0	$2.72 \cdot 10^{-3}$	$1/$MPa s
	c_1	1.98	MPa

Table 1: Material parameters of concrete

Numerical results are compared to the experimental results and to the results of numerical simulation presented by Gawin et al. [3] (Case 0) in Figure 2. Two cases are considered. In the first one (Case 1), sorption isotherm given by (25) which are the same as are used in work [3], are applied. Since material parameters in this model are difficult to experimentally define, sorption isotherms represented by (26, 27) whose parameters depend solely on the mixture properties are employed in the second case (Case 2).

The results compared in Figure 2 show good agreement, which indicates the adequacy of the applied model. Using different mathematical functions to model adiabatic temperature rise (equation given in work [3] for case 0 and Equation (11) for cases 1 and 2) cause slightly different values of temperature, but temperature rises of cases 1 and 2 are almost the same, from which it can be concluded that the type of sorption isotherm used does not affect temperature distribution. However, relative humidity is influenced by the sorption isotherms, but the results are still close enough.

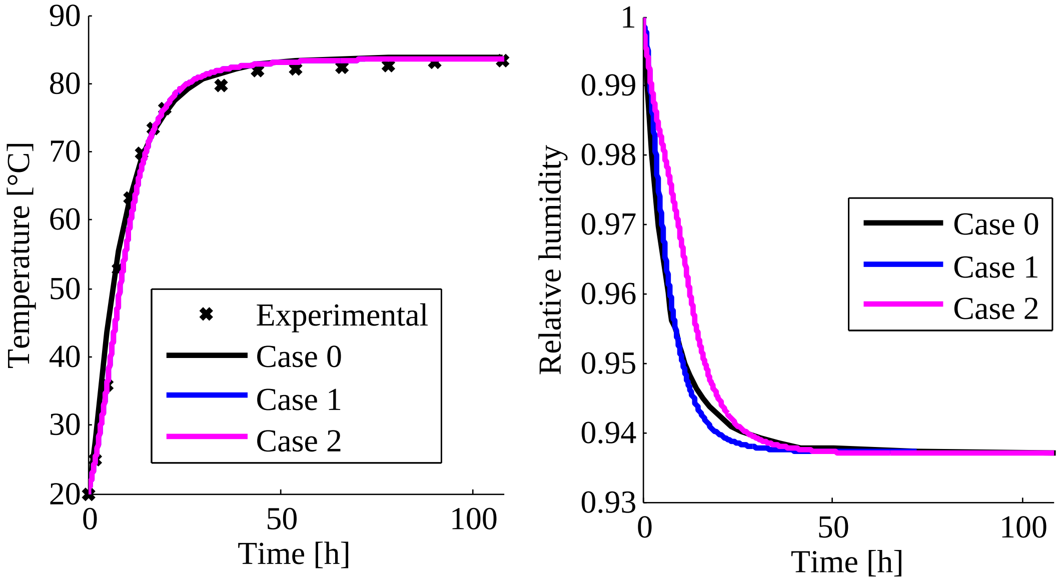

Figure 2: Comparison of experimental and numerical results

6 Conclusion

The numerical procedure for modelling fully coupled thermal, hygral and mechanical behaviour of concrete at early ages has been presented. Concrete has been treated as the porous material, composed of the solid skeleton and pores, filled with liquid water and moist air. Hydration of cement which causes temperature rise and desiccation of concrete has been taken into account as an internal heat source. Strains have been connected to the effective stresses, what holds for the creep strains modelled by microprestress-solidification theory as well. The set of partially differential governing equations has been solved iteratively by a finite element method.

A numerical example dealing with adiabatic test has been made. Good agreement between experimental and numerical results has shown adequacy of the proposed model. In addition to the sorption isotherms suggested in work [3], calculation was repeated using different sorption isotherms (26, 27) having parameters which are easier to determine. Getting results which do not differ much from the original one, the novel sorption isotherms have proved to be adequate as well.

Acknowledgements

Operation is part financed by European union, European social fund, and Ministry of education, science, culture and sport.

References

[1] M. Cervera, J. Oliver, T. Prato, "Thermo-Chemo-Mechanical model for concrete I: Hydration and aging", Journal of engineering mechanics, 125, 9, 1018-1027, 1999.

[2] R. T. Tenchev, L. Y. Li, J. A. Purkiss, "Finite element analysis of coupled heat and moistrure transfer in concrete subjected to fire", Numerical heat transfer, Part A, 39, 685-710, 2001.

[3] D. Gawin, F. Pesavento, B. A. Schrefler, "Hygro-thermo-chemo-mechanical modelling of concrete at early ages and beyond. Part I: Hydration and hydrotermal phenomena", International journal for numerical methods and engineering, 67, 299-331, 2006.

[4] D. Gawin, F. Pesavento, B. A. Schrefler, "Hygro-thermo-chemo-mechanical modelling of concrete at early ages and beyond. Part II: Shrinkage and creep of concrete", International journal for numerical methods and engineering, 67, 332-363, 2006.

[5] C. T. Davie, C. J. Pearce, N. Bićanić, "A fully generalised, coupled, multi-phase, hygro-thermo-mechanical model for concrete", Materials nad structures, 43, 13-33, 2010.

[6] M. Hassanizadeh, W. G. Gray, "General conservation equations for multi-phase systems: 1. Averaging procedure", Advances in water resources, 2, 131-144, 1979.

[7] M. Hassanizadeh, W. G. Gray, "General conservation equations for multi-phase systems: 2. Mass, momenta, energy and entropy equations", Advances in water resources, 2, 191-203, 1979.

[8] M. Hassanizadeh, W. G. Gray, "General conservation equations for multi-phase systems: 3. Constitutive theory for porous media flow", Advances in water resources, 3, 25-40, 1980.

[9] R. W. Lewis, B. A. Schrefler, "The finite element method in the static and dynamic deformation and consolidation of porous media (2nd edn)", Wiley, Chichester, United Kingdom, 1998.

[10] C. Ammar, P. Dutron, H. Motteu, J. Dubois, "La progression des betons et des mortiers par basses temperatures", C.S.T.C. - C.R.I.C. - SECO, Bruxelles, 1973.

[11] O. M. Jensen, P. F. Hansen, "Water entrained cement-based materials, I. Principles nad theoretical background", Cement and concrete research, 31, 647-654, 2001.

[12] P. Halamickova, R. J. Detwiler, "Water permeability and chloride ion diffusion in portland cement mortars: Relationship to sand content and critical pore diameter", Cement and concrete research, 25, 780-802, 1995.

[13] V. Boel, K. Audenaert, G. De Schutter, "Gas permeability and capillary porosity of self-compacting concrete", Materials and Structures, 41, 1283-1290, 2008.

[14] S. Zhang, M. Zhang, "Hydration of cement and pore structure of concrete cured in tropical environment", Cement and Concrete Research, 36, 1947-1953, 2006.

[15] V. Baroghel-Bouny, M. Mainguy, T. Lassabatere, O. Coussy, "Characterization

and identification of equilibrium and transfer moisture properties for ordinary and high performance cementitious materials", Cement and concrete research, 29, 1225-1238, 1999.

[16] D. Gawin, C. E. Majorana, B. A. Schrefler, "Numerical analysis of hygro-thermic behaviour and damage of concrete at high temperature", Mechanics of Cohesive-Frictional Materials, 4, 37-74, 1999.

[17] T. Hozjan, "Nonlinear analysis of composite planar structures exposed to fire", PhD thesis (in Slovene), University of Ljubljana, Faculty of Civil and Geodetic Engineering, 2009.

[18] D. Gawin, F. Pesavento, B. A. Schrefler, "Modelling of hygro-thermal behaviour of concrete at high temperature with thermo-chemical end mechanical material degradation", Computer methods in applied mechanics and engineering, 192, 1731–1771, 2003.

[19] Z. P. Bažant, A. B. Hauggaard, S. Baweja, F.-J. Ulm, "Microprestress-solidification theory for concrete creep. I: Aging and drying effects", Journal of Engineering Mechanics (ASCE), 123(11), 1188-1194, 1997.

[20] Z. P. Bažant, A. B. Hauggaard, S. Baweja, "Microprestress-solidification theory for concrete creep. II: Algorithm and verification", Journal of Engineering Mechanics (ASCE), 123(11), 1195-1201, 1997.

[21] Z. P. Bažant, S. Prasannan, "Solidification theory for concrete creep. II. Verification and application", Journal of Engineering Mechanics (ASCE), 115, 1704-1725, 1989.

[22] Z. P. Bažant, Y. Xi, "Continuous Retardation spectrum for solidification theory of concrete creep", Journal of engineering mechanics (ASCE), 121, 281-288, 1995.

[23] Z. P. Bažant, S. Prasannan, "Solidification theory for concrete creep. I: Formulation", Journal of Engineering Mechanics (ASCE) 115, 1691-1703, 1989.

[24] Z. P. Bažant, S. Baweja, in collaboration with RILEM Committee TC 107-GCS, "Creep and shrinkage prediction model for analysis and design of concrete structures – model B3", Materials and Structures, 28, 357-365, 1995.

[25] D. P. Bentz, V. Waller, F. de Larrard: "Prediction of adiabatic temperature rise in conventional and high-performance concrete using a 3-D microstructural model", Cement and concrete research, 28, 285-297, 1998.